European Journal of Cancer 229 (2025) 115755

Contents lists available at ScienceDirect

European Journal of Cancer

journal homepage: www.ejcancer.com

Original Research

Tumour microenvironment heterogeneity in primary and metastatic paired melanoma samples and its correlation with genetic features and prognosis

Mario Mandalà [a], Filippo Ugolini [b], Lorenzo Caldirola [c], Eliana Rulli [c], Antonella Manca [d,e], Maria Cristina Sini [d,e], Sara Simi [f], Gianna Baroni [f], Silvia Costabile [a], Vincenzo De Giorgi [g], Antonio Cossu [h], Guido Bellezza [i], Antonio Guadagno [j], Francesco Spagnolo [o], Andrea Gianatti [k], Paola Ghiorzo [l,m], Giuseppe Palmieri [d,e,1], Daniela Massi [f,n,*,1]

[a] *Unit of Medical Oncology, Department of Medicine and Surgery, University of Perugia, Perugia 06156, Italy*
[b] *Histopathology and Molecular Diagnostics, Careggi University Hospital, Florence 50139, Italy*
[c] *Methodology for Clinical Research Laboratory, Clinical Oncology Department, Istituto di Ricerche Farmacologiche Mario Negri IRCCS, Milan 20156, Italy*
[d] *Unit of Cancer Genetics, Institute of Genetic Biomedical Research (IRGB), National Research Council (CNR), Sassari 07100, Italy*
[e] *Immuno-Oncology & Targeted Cancer Biotherapies, University of Sassari, Sassari 07100, Italy*
[f] *Section of Anatomic Pathology, Department of Health Sciences, University of Florence, Florence 50139, Italy*
[g] *Section of Dermatology, Department of Health Sciences, University of Florence, Florence 50139, Italy*
[h] *Department of Medical, Surgical and Experimental Sciences, University of Sassari, Sassari 7100, Italy*
[i] *Section of Anatomic Pathology and Histology, Department of Medicine and Surgery, University of Perugia, Perugia 06156, Italy*
[j] *U.O. Anatomia Patologica Ospedaliera, IRCCS Ospedale Policlinico San Martino, Genoa 16132, Italy*
[k] *Unit of Pathology, Department of Oncology and Hematology, Papa Giovanni XXIII Hospital, Bergamo 24127, Italy*
[l] *Cancer Genetics, IRCCS Ospedale Policlinico San Martino, Genoa 16132, Italy*
[m] *Department of Internal Medicine and Medical Specialities, University of Genoa, 16132, Italy*
[n] *Department of Molecular Pathobiology, New York University - College of Dentistry, New York, NY 10010, USA*
[o] *IRCCS Ospedale Policlinico San Martino, Skin Cancer Unit, Genoa, Italy*

ARTICLE INFO

Keywords:
Melanoma
Inflamed
Non-inflamed
Heterogeneity
Gene expression profile

ABSTRACT

Background: The prognostic impact of tumour microenvironment (TME) heterogeneity in primary cutaneous melanomas (CM) and paired distant metastases is unclear. Few studies have explored the impact of genetic features on TME immune cell distribution. This study assessed the prognostic impact of TME heterogeneity and investigated the correlation between genetic features and TME cell composition.

Methods: Demographics, treatments and outcome of melanoma patients - with paired samples - from five Italian Melanoma Intergroup (IMI) centers were collected.

TME immune phenotypes and cell distribution in FFPE whole tumour sections were analyzed using 9 biomarkers (CD3, CD4, CD8, CD20, CD68, CD163, PD-1, PD-L1, FOXP3), classifying samples as desert (D), excluded (E), or inflamed (I). Additionally, genomic pathways were assessed by next-generation sequencing in both primary and paired samples.

Results: TME was evaluated in 221 samples from 91 patients.The distribution of immune phenotype (I vs E/D) of CD8 + cells ($p < 0.0001$), CD163 + cells ($p < 0.0001$), CD20 + cells ($p = 0.0008$), CD3 + cells ($p < 0.0001$), CD4 + cells ($p < 0.0001$), CD68 + cells ($p < 0.0001$), PD1 + cells ($p = 0.00015$) significantly differed between metastatic and primary melanomas.

In primary tumors, BRAFV600 status did not correlate with immune phenotypes. However, in paired metastases, it was inversely associated with infiltration of CD8 +, CD3 +, CD68 +, and CD20 + cells. Patients in the CD8 + D/E TME group had significantly shorter median survival (21 months) compared to those with at least one inflamed (I) TME sample [(58 months); HR 2.35, 95 % CI 1.28–4.32].

Conclusions: Metastatic and primary melanomas show distinct immune phenotypes. Longitudinal TME assessment predicts overall survival.

* Correspondence to: Section of Pathological Anatomy, Department of Health Sciences, University of Florence, Viale Pieraccini 6, Florence 50139, Italy.
E-mail address: daniela.massi@unifi.it (D. Massi).
[1] Equally contributed senior authorship.

https://doi.org/10.1016/j.ejca.2025.115755
Received 29 July 2025; Received in revised form 28 August 2025; Accepted 1 September 2025
Available online 8 September 2025

1. Introduction

The use of monoclonal antibodies blocking immunologic checkpoints has paved the way in cancer treatment [1]. Specifically, immune checkpoint inhibitors (ICIs) targeting cytotoxic T lymphocyte-associated protein 4 (CTLA-4) or programmed cell death protein 1 (PD-1) receptor expressed on T cells or its primary ligand programmed cell death ligand 1 (PD-L1) expressed on tumours or immune cells, have demonstrated remarkable antitumor activity and durable response in patients with advanced melanoma, thus improving prognosis and long-term survival outcomes [1]. Anti PD-1 antibodies have also revolutionized the way we treat patients with high-risk stage II (IIB-IIC) and III disease, reducing the absolute risk of recurrence by 15–20 % [2]. However, a substantial proportion of patients experiences limited benefit from immunotherapy, due to the presence of primary, adaptive or acquired resistance mechanisms [3].

The composition of the tumour microenvironment (TME) and the spatial distribution of CD8 + cells have been linked with prognosis in primary melanoma, regardless of ICI exposure. Additionally, intratumoral high density of CD8 + cells has been associated with improved response to ICIs [4]. Several studies have demonstrated that tumour infiltrating lymphocytes (TILs) serve as significant prognostic indicators in primary melanomas [5]. Furthermore, immune cell infiltrates in melanoma metastases also hold prognostic value; patients with melanoma metastases lacking intra-tumoral immune cell infiltration tend to have the poorest survival outcomes [6].

Historically, four subtypes of TME based on the presence or absence TILs and PD-L1 expression, have been identified (i.e. type I, TIL+/ PD-L1+: adaptive immune resistance; type II, TIL-/PD-L1+: immunological ignorance; type III, TIL-/PD-L1+: intrinsic induction; type IV, TIL+/PD-L1-: tolerance) with different responses to ICIs and patient outcome [7]. Immunologically “cold” tumours are characterized by a lack or a low number of TILs, which may result from low neoantigen load (i.e. tumour mutational burden, TMB), defective antigen presentation, or physical barriers that hinder lymphocyte migration in the TME [7,8]. For this reason, the therapeutic impact of immunotherapy is generally minimal in patients with immunologically “cold” tumours and their prognosis is poor, whereas in patients with “hot” tumours immunotherapy is therapeutically impactful and prognosis is generally favourable [6,9]. Nevertheless, the binary classification of patients into “hot” vs “cold” immune contexture in melanomas is complicated by potential intertumoral heterogeneity. The classification of TME in primary tumours compared to metastases, as well as the differences in cell composition among different local and distant metastatic sites has been inadequately investigated. Furthermore, the influence of genetic features on the TME remains unclear.

The aim of this study was to investigate TME heterogeneity in primary and paired metastatic melanoma samples and to explore its correlation with genetic features and clinical outcome.

2. Materials and methods

2.1. Study cohort

We investigated immune contexture in primary cutaneous melanomas (CM) and paired metastases in melanoma patients diagnosed, treated, and followed up prospectively in five Italian centres. The clinical and histopathological parameters extracted from the database included: gender, date of birth, date of diagnosis, anatomical site, histotype, Breslow thickness, ulceration, mitotic rate, TILs, sentinel lymph node (SLN) status, site of metastasis, date of metastasis, and follow-up including patient’s treatment and outcome. Formalin-fixed paraffin-embedded (FFPE) tissue sections, 3 μm in thickness, were stained with hematoxylin & eosin and reviewed to confirm the histopathological diagnosis and to assess tissue quality control. The use of formalin-fixed, paraffin-embedded sections of human samples was approved by the local Ethics Committee (13676_bio; Comitato Etico Regione Toscana-Area Vasta Centro) according to the Declaration of Helsinki".

3. Immunohistochemistry

Immunohistochemistry (IHC) was performed on representative FFPE whole tumor section 3-μm thick, using different combination of 9 cell biomarkers (CD3, CD4, CD8, CD20, CD68, CD163, PD-1, PD-L1 and FOXP3). We tested the following bright field (BF) multiplex IHC protocols: CD20/CD3, CD68/CD4, CD163/CD8, PD-L1/PD1 and FOXP3. For all multiplex protocols, sections were deparaffinized in EZ prep (#950–102; Ventana), and antigen retrieval was achieved by incubation with cell-conditioning solution 1 (#950–124; Ventana), a Tris ethylenediaminetetraacetic acid-based buffer (pH 8.2). Sections were incubated with the following primary antibodies: anti-CD3 (#790–4341, rabbit monoclonal, clone 2 G, V6 ready to use, Ventana Medical System, Tucson, AZ), anti-CD4 (#790–4423, rabbit monoclonal, clone SP35, ready to use, Ventana Medical System, Tucson, AZ), anti-CD8 (#790–4460, rabbit monoclonal, clone SP57, ready to use, Ventana Medical System, Tucson, AZ), anti-CD20 (#760–2531, rabbit monoclonal, clone L26, ready to use, Ventana Medical Systems, Tucson, AZ), anti-CD68 (#05721679001, mouse monoclonal, clone PGM1, ready to use, Diagnostic BioSystem, Pleasanton, CA), anti-CD163 (#760–4437, mouse monoclonal, clone MRQ-26, ready to use, Ventana Medical Systems, Tucson, AZ), anti-PD-L1 (#13684S, clone, E1L3N, rabbit monoclonal, 1:50, Cell signalling Danvers, Massachusetts), anti-PD-1 (#07099029001, clone NAT105, ready to use, Ventana Medical Systems, Tucson, AZ) and anti-FOXP3 (clone 236A/E7, #14–477–82, mouse monoclonal, 1:60, Invitrogen, Waltham, Massachusetts).

Each denaturation step was done by treating slides with Ultra CC2 (#950–223, ready to use, Ventana Medical Systems, Tucson, AZ) for 8 min at 100°C (Ugolini 2022). The signal was developed with anti-mouse or anti-rabbit Alk Phos (AP) and anti-mouse or anti-rabbit HRP coupled with the following chromogens: DISC. PURPLE Kit (#760–229, ready to use, Ventana Medical Systems, Tucson, AZ) for: CD20, CD68, CD163, PD-L1; DISC. YELLOW Kit (#760–239, ready to use, Ventana Medical Systems, Tucson, AZ) for: CD3, CD4, CD8, and PD1. Chromomap RED (#760–160, ready to use, Ventana Medical Systems, Tucson, AZ) was used for FOXP3. Sections were counterstained with Hematoxylin II (#790–2208, ready to use, Ventana Medical Systems, Tucson, AZ, read).

IHC staining were semi-quantitative scored as following: 0–3 + for intratumoral and 0–3 + for peritumoral areas (score 0: absence of stained cells; score 1: 1–10 %; score 2: 11–50 %; score 3: >50 %); PD-L1 was scored as percentage of positive melanoma cells and intratumoral/peritumoral immune cells (ICs). In addition, for the all immune cells studied, we applied the CD8 + cells classification as follows: absence of immune cells into the parenchyma, desert tumours (D); accumulation of immune cells at the invasive margin or in the intratumoral stroma without effective invasion into the parenchyma, excluded tumors (E); and infiltration of immune cells into the tumour parenchyma, in inflamed tumors (I) as previously proposed by Sobottka and colleagues [10].

The immunohistochemical evaluation was performed in intratumoral and peritumoral areas, separately. In assessing the peritumoral tissue, we focused on the contact surface between the invasive margin and the surrounding healthy tissue. The microscopic evaluation of peritumoral margins were conducted by two expert dermatopathologists, ideally considering a thickness of approximately 500 μm across the lesion margin, as previously defined [11,12]. Importantly, the most inflamed areas were not specifically selected; instead, the assessment was carried out comprehensively across the whole tumor area, both in primary melanomas and in the paired metastases. This strategy ensured the application of a uniform evaluation criteria to both primary lesions and paired metastases, where the distinction between superficial and deep areas is not always feasible. In addition, to account for potential

differences in the spatial distribution of immune cells, we applied the classification proposed by Sobottka and colleagues [10]. This complementary analysis allowed us to assess not only the density, but also the spatial distribution of immune cells.

4. Genetic analysis

For genetic analysis, genomic DNA was isolated from 7 mm thick formalin-fixed and paraffin-embedded (FFPE) tissue sections with QIAamp DNA FFPE Advanced UNG Kit, (©Qiagen, Hilden, Germany) QIAGEN, DNA concentrations were assessed by Qubit 2.0 Fluorometer with Qubit dsDNA HS (High Sensitivity) Assay Kit (Life Technologies, Carlsbad, CA, USA). Next generation sequencing (NGS) analyses were performed using the Ion GeneStudio S5 Prime System and carried out by Oncomine™ Comprehensive Assay (OCA) Plus DNA Manual kit (Thermo Fisher Scientific Inc) which provides a comprehensive genomic profiling solution The data analysis workflow was performed by automated data transfer from the Ion Torrent™ Server (Thermo Fisher Scientific Inc) to the Ion Reporter™ Server (Thermo Fisher Scientific Inc) for variant analysis using the panel specific workflow. Bioinformatic data analysis included Tumour Mutation Burden (TMB), CNVs evaluation and Loss of Heterozygosity assessment (LOH). The variants have been filtered using the following parameters: >100x coverage, 5 %<mutant allele frequency< 95 %, variant type= SNV, MNV, CNV. Only genes strictly related to melanoma pathogenesis as MAPK, PI3K/AKT, INK/ARF, TP53, NOTCH, WNT pathways, JAK, STAT, ARID, TERT promoter were considered. Each variant was investigated for its potential pathogenic role using prediction algorithms SIFT (Sorting Intolerant From Tolerant) and PolyPhen-2 (Polymorphism Phenotyping v2) integrated in the Ion Reporter™ software, and the publicly available databases Catalogue Of Somatic Mutations In Cancer (COSMIC) (https://cancer.sanger.ac.uk/cosmic), the Single Nucleotide Polymorphism Database (dbSNP) (https://www.ncbi.nlm.nih.gov/snp/), ClinVar (https://www.ncbi.nlm.nih.gov/clinvar/) and the Genome Aggregation Database (gnomAD) (https://gnomad.broadinstitute.org).

In addition, some bioinformatics softwares such as VarSome (https://varsome.com/), InterVar (https://wintervar.wglab.org/about.php) and Franklin by Genoox (https://franklin.genoox.com/clinical-db/home), able to perform clinical interpretation of genetic variants according to the ACMG guideline for variant classification categories: "Benign", "Likely Benign", "Uncertain Significance", "Likely Pathogenic" and "Pathogenic", were used to assess the potential pathogenicity of all the identified sequence variants.

5. Statistical analysis

Continuous variables were described using mean and standard deviation (SD), median with the first and third quartiles (Q1-Q3) and minimum and maximum values, whereas categorical variables were described using frequencies and percentages.

The chi-squared test (or Fisher's exact test, where appropriate) was used to measure the association between the categorical variables. Since this analysis included comparisons between multiple measurements made on the same patient, methods for repeated measures were implemented. When comparisons were carried out between primary tumour and paired metastases, if multiple metastases were present for the same patient, all metastases were considered. When we compared the primary tumour with the first metastatic sample, only the first available site of recurrence was considered. Differences between TME and genetical features in metastases and primary tumour were assessed using logistic models for repeated measures. Friedman test was used to investigate the differences between metastatic sites in terms of immune phenotypes.

The overall survival (OS) was defined as the interval between the date of primary tumour diagnosis and death for any cause. For alive patients at time of this analysis, survival data were right censored to the date of last information available. Survival distributions were estimated by the Kaplan Meier (KM) method, described by means of median survival and 95 % confidence intervals (95 % CIs) and compared using the log-rank test.

6. Results

The cohort included 91 primary CM with 130 paired metastases from five Italian centres: S. Martino Hospital, Genova n = 40; University of Florence n = 18; University of Sassari n = 17; Papa Giovanni XXIII Hospital Bergamo n = 3, and S.M. della Misericordia Hospital Perugia n = 13.

Demographic and clinical characteristics of patient cohort are summarized in Table S1. Among the 91 retrieved patients, 56.0 % were male, and the median age at diagnosis was 64.2 years (Q1-Q3: 51.8–77.5). Superficial spreading melanoma, nodular melanoma and acral melanoma were diagnosed in 49.5 %, 21.6 %, 20.5 % of cases, respectively. The median Breslow thickness was 4.2 mm, most of them were ulcerated (61.5 %). At the time of diagnosis 33 patients (36.3 %) were with stage I-II, 49 patients (53.8 %) with stage III, 6 patients (6.6 %) with stage IV and for 3 patients (3.3 %) stage was not available. At the time of inclusion to the present study, all patients had metastatic disease, 16.5 % with M1d disease (15 patients), 24.2 % with M1c disease (22 patients), 15.4 % with M1b disease (14 patients), 44.0 % with M1a disease (40 patients). Metastatic sites were categorized into three groups: skin, lymph nodes, visceral/lung. Visceral metastases included stomach, bowel, adrenal gland and 1 brain metastasis. Overall, 23 (25.0 %) and 2 patients (2.2 %) received inhibitors of Braf and Mek (BRAFi/MEKi) as 1st- or 2nd-line therapy, respectively, and 25 (27.2 %) and 7 patients (7.6 %) received ICI as 1st- or 2nd-line therapy. Six patients were metastatic at the time of diagnosis, for the remaining patients the median time from diagnosis to metastatic disease was 6.2 months (Q1 - Q3: 1.8 – 30.8 months). A total of 29 patients received a diagnosis of metastasis more than a year after the primary diagnosis, with a maximum of 13 years.

Overall, 130 paired samples from 91 patients were analyzed, among them 75 (82.4 %) patients had 1 metastasis, 8 (8.8 %) 2 metastases, 3 (3.3 %) 3 metastases, 3 (3.3 %) 4 metastases, 1 patient (1.1 %) 7 metastases and 1 (1.1 %) patient had 11 metastases. Anatomical location of 130 metastatic sites: skin/subcutis n = 60 (46.2 %), lymph nodes n = 54 (41.5 %), lung (n = 5) and other visceral sites (stomach=4, bowel n = 5, adrenal gland n = 1, brain n = 1) (lung + visceral n = 16, 12.3 %).

TME assessment was performed in 219 samples from 90 patients (1 paired sample not evaluable). Immune phenotypes evaluated in primary melanoma and paired metastases is shown in Fig. S1.

Description of immune phenotypes and their pattern of distribution (intratumoral and peritumoral) in primary tumours and metastases are reported in Table S2, S3. In the metastatic samples, the expression of PD-L1 was associated with the inflamed immunophenotype of CD20 + cells ($p = 0.0037$), CD3 + cells ($p = 0.0075$), CD4 + cells ($p = 0.0081$), CD8 + cells ($p = 0.0151$), FOXP3 + cells ($p = 0.0090$) (Table S4).

To investigate the potential heterogeneity of TME, primary tumours and paired metastases were compared in terms of immune phenotypes distribution. Table 1 summarizes the main results. Specifically, the immune phenotype distribution (I vs E/D) of CD8 + cells ($p < 0.0001$), CD163 + cells ($p < 0.0001$), CD20 + cells ($p = 0.0008$), CD3 + cells ($p < 0.0001$), CD4 + cells ($p < 0.0001$), CD68 + cells ($p < 0.0001$), PD1 +cells ($p = 0.00015$) were significantly different in metastatic samples compared to primary melanoma (Fig. 1). Table 2 shows the logistic regression model comparing immunological phenotypes in primary vs metastasis according to metastatic sites. Briefly, the result above showing a different immune phenotype distribution between primary and metastatic samples were confirmed for all the three metastatic sites except for CD20 + cells that did not differ in primary vs skin metastases and for PD1 that show different immunological phenotype only for primary vs lymph nodes.

To investigate the potential heterogeneity in cell composition and

Table 1
Logistic regression model comparing immunological phenotypes in primitive vs metastases (adjusting for subject).

	OR	CI-	CI+	p-value
CD163 (I vs D,E)	5.2031	2.7217	9.9469	< .0001
CD20 (I vs D,E)	3.5937	1.7242	7.4900	0.0008
CD3 (I vs D,E)	3.4950	1.9774	6.1775	< .0001
CD4 (I vs D,E)	3.3993	1.9275	5.9948	< .0001
CD68 (I vs D,E)	5.7152	2.7680	11.800	< .0001
CD8 (I vs D,E)	3.4611	1.9649	6.0967	< .0001
PD1 (I vs D,E)	6.4777	2.0743	20.229	0.0015
FOXP3 (I vs D,E)	1.2846	0.6172	2.6735	0.5002
CD8 I / CD163 I (vs I/ D,E)	2.7143	0.8585	8.5816	0.0891
CD8 D,E/ CD163 D,E (vs I/ D,E)	0.5031	0.1551	1.6323	0.2526
CD8 D/E / CD163 I (vs I/ D,E)	3.1111	0.5585	17.330	0.1952

Legend: N: number of patients; D: desert; E: excluded; I: inflamed OR: odds ratio; CI: confidence interval

pattern of distribution among metastatic sites, we compared skin, lymph nodes, lung/visceral metastases. Interestingly, the immune phenotype distribution pattern was similar among these metastatic sites (Table 3), that is, the immune phenotype distribution and composition was not different in skin, lymph nodes, lung/visceral metastatic sites. Given the heterogeneity of primary melanoma and metastatic sites, we interrogated our dataset to understand whether the first site of metastatic disease could match with metachronous metastases in terms of cell composition and pattern of distribution. Indeed, we found that the primary metastatic site mirrored the different immune phenotype pattern distribution between primary and metastatic sites (Table 4).

7. Correlation between genetic and TME features in paired samples

Genomic assessment was available for 178 samples from 79 patients. A panel of genomic pathways was tested, by NGS, on primary CM and paired metastases, including MAPK pathway activation with or without NRAS/BRAF mutation (65 patients, 82.3 %), PI3K/AKT (16 patients,

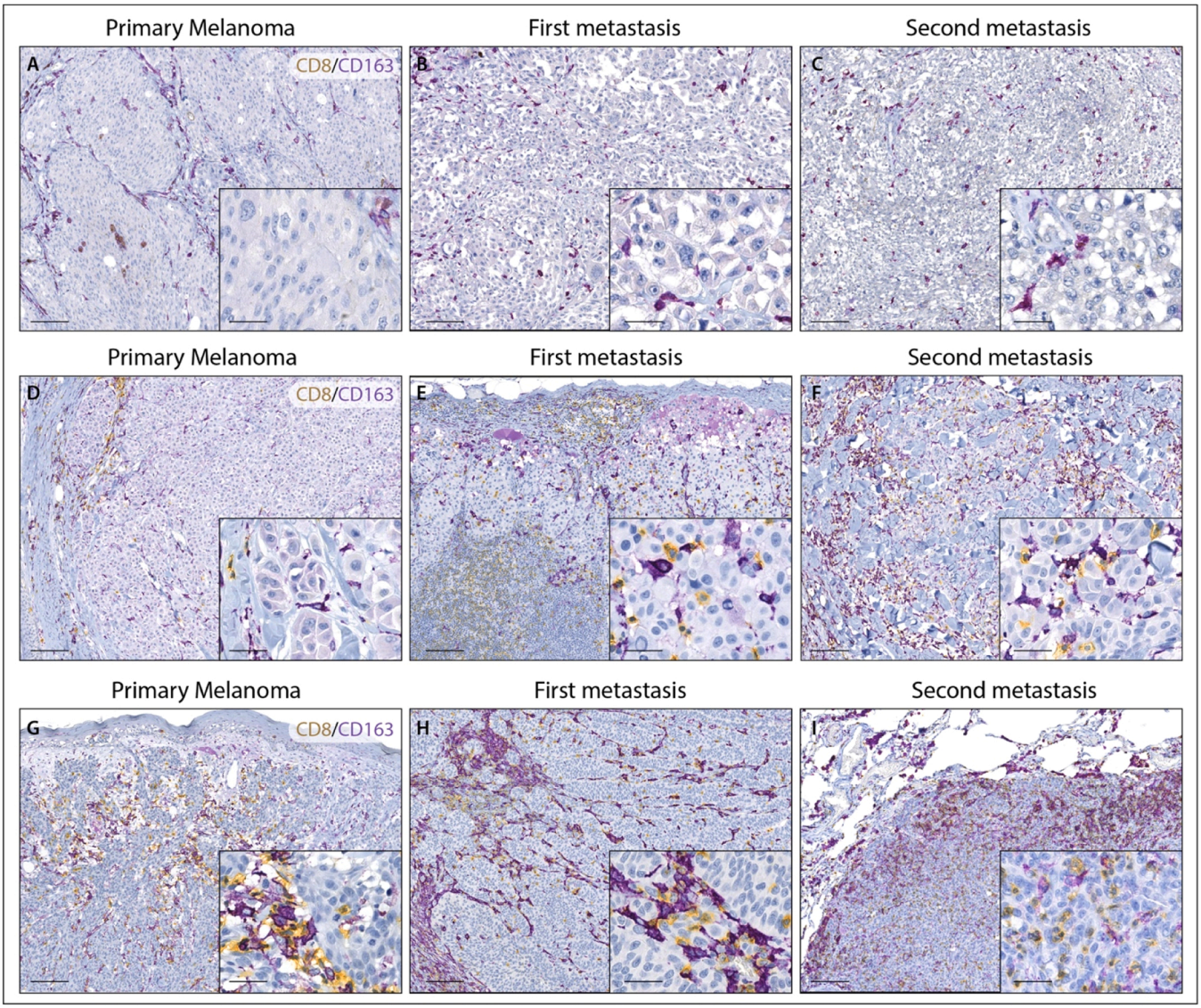

Fig. 1. Representative images of TME in primary and metastatic melanoma samples. Double immunohistochemical analysis with anti-CD8/CD163 antibodies showing an immune-desert primary melanoma (A) and concordant immune-desert paired metastases (B-C); immune-excluded TME in primary melanoma (D) switching to immune-inflamed TME in the respective metastases (E-F); concordant immune-inflamed TME in primary (G) and paired metastases shows abundant infiltration of immune cells in the tumor mass (H-I). Original magnification 10x, inset 40x; scale bar 100μm and 25μm respectively.

Table 2
Logistic regression model comparing immunological phenotypes in primitive vs metastasis (adjusting for subject) according to metastasis site.

	Skin				Lymph nodes				Visceral/lung			
	OR	CI-	CI+	p	OR	CI-	CI+	p	OR	CI-	CI+	p
CD163 (I vs D,E)	5.6841	2.4696	13.083	0.0001	5.8142	2.1304	15.868	0.0009	4.3290	1.2502	14.990	0.0238
CD20 (I vs D,E)	1.7381	0.7633	3.9579	0.1839	9.4649	2.3007	38.939	0.0024	4.0325	1.2216	13.311	0.0251
CD3 (I vs D,E)	2.6409	1.3218	5.2767	0.0068	5.5850	2.0545	15.182	0.0011	4.3784	1.1790	16.259	0.0299
CD4 (I vs D,E)	2.5694	1.2899	5.1184	0.0081	6.7647	2.1330	21.453	0.0016	4.5834	1.2334	17.033	0.0259
CD68 (I vs D,E)	6.1251	2.4379	15.389	0.0002	6.8530	2.1628	21.714	0.0015	3.6882	1.0685	12.731	0.0402
CD8 (I vs D,E)	2.8148	1.4088	5.6241	0.0041	4.2236	1.8282	9.7579	0.0011	4.6667	1.2565	17.332	0.0244
PD1 (I vs D,E)	3.1523	0.7938	12.518	0.1010	6.0869	1.7673	20.964	0.0050	14.027	0.3620	543.51	0.1446
FOXP3 (I vs D,E)	0.9264	0.3784	2.2680	0.8648	1.9361	0.6838	5.4821	0.2083	0.5506	0.0580	5.2291	0.5804
CD8 I / CD163 I (vs I/ D,E)	6.2834	0.7303	54.065	0.0942	1.6000	0.4658	5.4961	0.4554	NE	NE	NE	NE
CD8 D,E/ CD163 D,E (vs I/ D, E)	1.3580	0.1512	12.200	0.7847	0.3019	0.0818	1.1142	0.0722	NE	NE	NE	NE
CD8 D/E / CD163 I (vs I/ D,E)	10.663	0.8231	138.14	0.0701	1.6000	0.2272	11.266	0.6369	NE	NE	NE	NE

Legend: D: desert; E: excluded; I: inflamed; OR: odds ratio; CI: confidence interval; p: p-value; NE: not estimable
*visceral metastases include metastases located in stomach, colon, small intestine, adrenal gland and brain

Table 3
Comparison of immune phenotypes among metastatic sites (skin, lymph nodes, lung/visceral*).

	p-value (friedman test)
CD163 (I vs D,E)	0.4949
CD20 (I vs D,E)	0.7273
CD3 (I vs D,E)	0.7617
CD4 (I vs D,E)	0.7617
CD68 (I vs D,E)	0.4550
CD8 (I vs D,E)	0.8263
PD1 (I vs D,E)	0.3272
FOXP3 (I vs D,E)	0.0592
CD8/CD163 combinations	0.6266

Legend: D: desert; E: excluded; I: inflamed, Visceral included: stomach, bowel, adrenal gland, only 1 brain metastasis was available

Table 4
Logistic regression model comparing immunological phenotypes in primitive vs first metastasis (adjusting for subject).

	OR	CI-	CI+	p-value
CD163 (I vs D,E)	5.2031	2.7217	9.9469	< .0001
CD20 (I vs D,E)	3.5937	1.7242	7.4900	0.0008
CD3 (I vs D,E)	3.4950	1.9774	6.1775	< .0001
CD4 (I vs D,E)	3.3993	1.9275	5.9948	< .0001
CD68 (I vs D,E)	5.7152	2.7680	11.800	< .0001
CD8 (I vs D,E)	3.4611	1.9649	6.0967	< .0001
PD1 (I vs D,E)	6.4777	2.0743	20.229	0.0015
FOXP3 (I vs D,E)	1.2846	0.6172	2.6735	0.5002
CD8 I / CD163 I (vs I/ D,E)	2.7143	0.8585	8.5816	0.0891
CD8 D,E/ CD163 D,E (vs I/ D,E)	0.5031	0.1551	1.6323	0.2526
CD8 D/E / CD163 I (vs I/ D,E)	3.1111	0.5585	17.330	0.1952

Legend: N: number of patients; D: desert; E: excluded; I: inflamed OR: odds ratio; CI: confidence interval

20.5 %), JAK 1–3 (19 patients, 24.1 %), INK4 ARF (17 patients, 21.5 %), STAT 1–3–5–6 (4 patients, 5.1 %), P53 (18 patients, 23.1 %), NOTCH (13 patients, 16.5 %), WNTARID (10 patients, 12.7 %), pTERT (43 patients, 58.9 %), as well as BRAFV600 (1 patient, 1.8 %), CDKN2A (13 patients, 22.4 %), PTEN pathway (17 patients, 29.3 %) as well as copy number variations (CNV). Furthermore TMB (mutations/Mb) was assessed in 87.3 % of patients. Tables S5, S6 summarize the main results in primary and paired metastases, while Table S7 summarizes the logistic regression model comparing pathway mutations in primitive vs metastasis.

All the genomic pathways, but JAK1–3 where a higher prevalence of the mutation was observed in primary sample respect to metastatic sites, were concordant between primary tumours and paired metastases.

Interestingly, while BRAFV600 mutation did not correlate with immune phenotypes features in the TME of primary melanoma, in paired metastases BRAFV600 mutation inversely correlated with CD8 + , CD3 + , CD68 + , CD20 + cell infiltration, hence BRAFV600 mutated metastatic samples correlated with an immune D/E phenotype compared to BRAF wild-type samples (Table S8).

8. Correlation between TME features in paired samples and outcome in patients receiving systemic therapy

Overall, 17 patients treated with anti-PD1 based therapy and 17 with BRAFi/MEKi had metastases available before starting treatment. Of these, 4 (1 with anti-PD1 based therapies, 3 with BRAFi/MEKi) had available metastases during treatment as well. All these patients also had available the primary tumour. Of the remaining patients treated with anti-PD1 based therapy or BRAFi/MEKi, 13 had available the primary sample (7 with anti-PD-1 based therapy, 6 with BRAFi/MEKi) and at least a metastatic sample during treatment, while one patient, treated with BRAFi/MEKi, had an available metastasis after stopping the treatment.

The median duration of the antitumor treatment in patients treated with immunotherapy or BRAFi/MEKi was 12.2 months (Q1 - Q3: 5.1 – 21.0 months).

Overall, 17 patients, who received BRAFi/MEKi or anti-PD1 based therapy in first line treatment, had available paired samples before and during systemic treatment. In the ICI group, TME composition in terms of CD163 + cells, CD3 + cells and CD8 +cells infiltration remained unchanged over time (longitudinally D/E) in two third of patients (6 patients, 66.7 %). All these patients experienced disease progression during treatment. In patients receiving BRAFi/MEKi 7 patients (87.5 %) exhibited a shift from D/E to I TME (Table S9).

We first evaluated the prognostic impact of the longitudinal TME composition during treatment by comparing OS between two groups in the overall population. One group included patients with a D or E CD8 + cells distribution in both the primary tumour and paired metastasis (N = 17) while the other comprised patients with at least one samples exhibiting an inflamed TME, as indicated by CD8 + cell infiltration (N = 73). The median OS was significantly shorter in the CD8 + D/E TME group−21.7 months (95 %CI 7.2–49.3)−compared to 58 months (95 %CI 41.5–70.3) in patients with at least one TME inflamed sample (HR 2.35, 95 %CI 1.28–4.32, p-value=0.0059) (Table S10), respectively (Fig. 2A).

The analysis on CD8 + phenotype was performed separately for patients treated with BRAFi/MEKi (N = 25) and those treated with ICI (N = 23). In patients receiving BRAFi/MEKi the D/E group had a significantly worse prognosis compared to patients with at least 1 TME inflamed sample (HR 7.36, 95 % CI 1.81–29.97) (Fig. 2B). Similar results were observed in those receiving ICI (HR 3.70 (95 % CI

1.17–11.73) (Fig. 2C).

There was no significant prognostic impact of CD163 + cells levels concerning the longitudinal TME assessment in the overall population (HR 0.66, 95 %CI 0.36–1.22, p-value=0.1859; Table S11 and Figs. S2–S4 both Supplementary) as well as within subgroups of patients treated with BRAFi/MEKi or anti-PD1 based therapy as first line therapy.

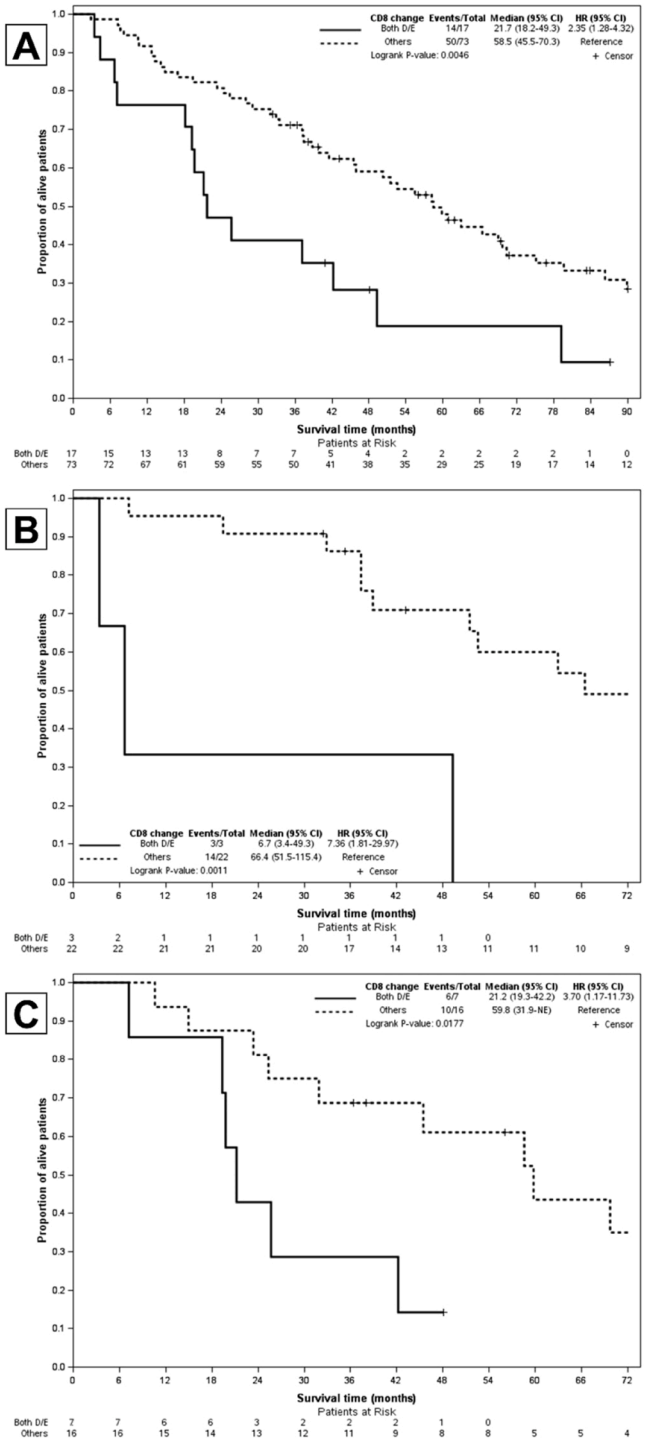

Fig. 2. OS Kaplan Meier curves by CD8 immunological phenotype: consistent D/E in all paired samples vs at least 1 inflamed paired sample in the whole population –(A); OS Kaplan Meier curves by CD8 phenotype change in patients treated with BRAFi/MEKi: consistent D/E in all paired samples vs at least 1 inflamed paired sample –(B); OS Kaplan Meier curves by CD8 phenotype change in patients treated with ICI: consistent D/E in all paired samples vs at least 1 inflamed paired sample –(C).

9. Discussion

Our study conveys 4 key messages: 1) the immune phenotype distribution (I vs D/E) based on CD8 + cells, CD163 + cells, CD20 + cells, CD3 + cells, CD4 + cells, CD68 + cells, PD1 + cells is significantly different in metastatic samples compared to primary melanomas; 2) the primary metastatic site mirrors the different immune phenotype pattern distribution between primary and metastases in skin, lymph-node and lung/visceral metastases; 3) in paired metastases BRAFV600 mutation inversely correlates with infiltration of CD8 +, CD3 +, CD68 +, CD20 + cells, whereas no association has been observed in primary melanoma; 4) longitudinal assessment of TME has prognostic value, correlating with OS.

It is well known that cancer is not simply the result of genetic alterations but rather a complex and dynamic ecosystem, involving non-cancerous cells and their interactions with cancer cells [4]. Previous studies have reported that high intratumoral density of CD8 + cells is associated with a better response to ICIs [6], and immune cell infiltrates in melanoma metastases are prognostic [6]. In this context, the results of our study are informative and extends these previous observations. Our results suggest that TME composition changes longitudinally during tumour progression and, as a consequence, classifying patients solely based on immune cell profile in primary melanoma may be not informative to prognosticate outcome. Indeed, our data show that by classifying TME in D/E vs I, cell composition changes significantly from primary melanoma to metastatic disease, indicating dynamic alterations over time. Our study complements recent studies showing that TME heterogeneity influences the behaviour of cancer cells through various biological mechanisms, including secretion of growth factors, cytokines, nutrient availability, hypoxia variations, and alterations in cancer metabolism [13–16]. Furthermore, pilot studies have reported that several immune-related genes exhibit different expression profiles in primary vs metastatic sites [17]. Overall, these findings suggest that, due to significantly heterogeneity in primary and metastatic sites, primary tumour samples may not accurately reflect the metastatic TME. Hence, in clinical studies, it would be advisable to examine the TME from a metastatic site instead of primary melanoma as this approach may be more informative to predict prognosis, response to treatment and, consequently, to potentially escalate or de-escalate treatment. Another worthwhile finding from our study is the importance of the longitudinal assessment of TME. Indeed, patients with D/E TME immunophenotype in both primary melanoma and metastatic sites showed the worst prognosis compared to patients with paired inflamed TME or with at least one of the samples showing a TME inflamed behaviour. This has consequences in the way we stratify patients in clinical trials, since the prognosis was different even in patients receiving, in the first line, BRAFi/MEKi as well as ICI. These findings identifying patients with consistent D/E TME immunophenotype may be important, since these patients should be candidate to experimental strategies with the aim to improve their prognosis. Furthermore, if these results were validated in independent series, TME status, longitudinally assessed could be a stratification factor in clinical studies.

We found that primary metastatic site mirrors the immune phenotype pattern distribution of other metastatic sites, mainly in skin, lymph node and lung. Recently Conway et al showed that patients with only liver, brain or bone metastases had significantly lower T-cell infiltration than lung and lymph nodal metastases [18]. Unfortunately, in our series, samples from liver and bone were lacking, and only one brain metastasis was available, preventing analysis of TME in these metastatic sites.

Consistent with other studies, patients who progressed during ICI treatment showed a D/E TME [19,20], while during the initial treatment with BRAFi/MEKi a switch from D/E CD8 + cells to inflamed CD8 + cells has been observed in majority of patients treated with targeted therapy with available paired samples obtained few weeks after

treatment initiation [21,22].

In our series, BRAFV600 mutation inversely correlated with CD8 + , CD3 + , CD68 + , CD20 + cell infiltration in metastatic samples. These results are consistent with translational studies showing that BRAFV600 mutant melanomas have a significantly more immunosuppressive TME characterized by lower major histocompatibility complex expression, reduced melanoma antigen expression, higher intratumorally regulatory T cells, and increased immunosuppressive cytokines [22–25]. Interestingly, in our cohort, BRAFV600 mutation from primary melanoma samples was not associated with an immunosuppressive TME behaviour. Overall, our results suggest that BRAF mutated metastatic samples rather than primary melanoma are associated with an immune D/E phenotype compared to BRAF WT samples. Whether the biological role of BRAFV600 mutation may be different in primary and metastatic melanoma warrants validation in independent series, ideally incorporating paired metastasis as in our study within controlled clinical trials. Since BRAFi/MEKi provide long term favourable response in early-stage disease and not in advanced disease, these findings may partially explain clinical trials outcomes. However, more robust, controlled studies are needed to validate and support our exploratory analysis.

Regarding the genomic profile, our study also shows that all pathways, except JAK1–3, were concordant between primary tumours and paired metastases. Consistent with previous studies, the suppression of the JAK3 pathway may play a crucial role in the migratory and invasive capacity of melanoma cells [26,27]; a factor that appears to be associated with a poorer prognosis in this patient group.

Our study has several strengths including: 1) a relatively large series with paired samples, 2) patients treated in the context of Italian Melanoma Intergroup centres, 3) centralized assessment of TME and genetic features; 4) we used conventional pathological assessment, easy to be implemented in pathology laboratories.

We acknowledge potential limitations of our study, including: 1) its retrospective design, which may introduce selection bias 2) the absence of samples from some metastatic sites, such as liver and bone, while only 1 brain metastases was available.

In summary, our study suggests not only a significant heterogeneity of immune phenotype distribution in metastatic samples compared to primary melanoma, but also a prognostic impact of the TME behaviour evaluated longitudinally in metastatic sites, since primary tumour samples may be unrepresentative of the metastatic TME behaviour. Furthermore, a different association of BRAFV600 mutation on TME behaviour in primary and metastatic samples has been found. Given the prognostic impact, our findings should be confirmed in independent for external validation.

CRediT authorship contribution statement

Caldirola Lorenzo: Visualization, Validation, Methodology, Formal analysis, Data curation. **Guadagno Antonio:** Resources, Data curation. **Ugolini Filippo:** Resources, Data curation. **De Giorgi Vincenzo:** Validation, Resources, Data curation, Conceptualization. **Costabile Silvia:** Visualization, Supervision, Data curation. **Bellezza Guido:** Resources, Methodology, Data curation. **Mandalà Mario:** Writing – review & editing, Writing – original draft, Validation, Supervision, Data curation, Conceptualization. **Cossu Antonio:** Validation, Resources, Methodology, Data curation, Conceptualization. **Palmieri Giuseppe:** Writing – review & editing, Resources, Funding acquisition, Data curation, Conceptualization. **Sini Maria Cristina:** Validation, Resources, Methodology, Data curation. **Ghiorzo Paola:** Validation, Resources, Data curation, Conceptualization. **Manca Antonella:** Resources, Data curation. **Baroni Gianna:** Supervision, Resources, Project administration, Data curation. **Massi Daniela:** Writing – review & editing, Validation, Supervision, Resources, Funding acquisition, Data curation, Conceptualization. **Simi Sara:** Supervision, Resources, Project administration, Data curation. **Gianatti Andrea:** Validation, Resources, Data curation, Conceptualization. **Rulli Eliana:** Visualization, Validation, Project administration, Formal analysis, Data curation. **Spagnolo Francesco:** Resources, Data curation.

Funding

The research has received funding from Fondazione AIRC under 5 per Mille 2018-ID.21073 project.

Declaration of Competing Interest

The authors declare that they have no known competing financial interests or personal relationships that could have appeared to influence the work reported in this paper.

Acknowledgements

Epigenetic Immune-oncology Consortium AIRC (EPICA) Investigators (Michele Maio, University of Siena, Italy, and Center for Immuno-Oncology, Department of Oncology, University Hospital of Siena, and NIBIT Foundation Onlus, Siena, Italy; Andrea Anichini, Department of Experimental Oncology, Fondazione IRCCS Istituto Nazionale dei Tumori, Milan, Italy; Ulrich Pfeffer, Laboratory of Gene Expression Regulation, IRCCS Ospedale Policlinico San Martino, Genua, Italy; Michele Ceccarelli, Sylvester Comprehensive Cancer Center, and Department of Public Health Sciences, Miller, School of Medicine, University of Miami, Miami, FL, USA; Luana Calabrò, Department of Translational Medicine, University of Ferrara, Ferrara, Italy and Division of Medical Oncology, Department of Medical Oncology, University Hospital of Ferrara, Ferrara, Italy; Beatrice Bodega, INGM, Istituto Nazionale di Genetica Molecolare 'Romeo ed Enrica Invernizzi, Milan, Italy and Department of Biosciences, University of Milan, Milan, Italy.

Appendix A. Supporting information

Supplementary data associated with this article can be found in the online version at doi:10.1016/j.ejca.2025.115755.

References

[1] Wolchok JD, Chiarion-Sileni V, Rutkowski P, et al. Final, 10-Year outcomes with nivolumab plus ipilimumab in advanced melanoma. N Engl J Med 2025;392(1):11–22.
[2] Garbe C, Amaral T, Peris K, et al. European consensus-based interdisciplinary guideline for melanoma. Part 2: treatment - update 2024. Eur J Cancer 2025;215:115153.
[3] Karasarides M, Cogdill AP, Robbins PB, et al. Hallmarks of resistance to Immune-Checkpoint inhibitors. Cancer Immunol Res 2022;10(4):372–83.
[4] Wong PF, Wei W, Smithy JW, et al. Multiplex quantitative analysis of Tumor-Infiltrating lymphocytes and immunotherapy outcome in metastatic melanoma. Clin Cancer Res 2019;25(8):2442–9.
[5] Hothem Z, Bayci A, Thibodeau BJ, et al. Using global gene expression to discriminate thin melanomas with poor outcomes. Mol Cell Oncol 2016;4(1):e1253527.
[6] Tumeh PC, Harview CL, Yearley JH, et al. PD-1 blockade induces responses by inhibiting adaptive immune resistance. Nature 2014;515(7528):568–71.
[7] Teng MW, Ngiow SF, Ribas A, et al. Classifying cancers based on T-cell infiltration and PD-L1. Cancer Res 2015;75(11):2139–45.
[8] Massi D, Brusa D, Merelli B, et al. The status of PD-L1 and tumor-infiltrating immune cells predict resistance and poor prognosis in BRAFi-treated melanoma patients harboring mutant BRAFV600. Ann Oncol 2015;26(9):1980–7.
[9] Ribas A, Shin DS, Zaretsky J, et al. PD-1 blockade expands intratumoral memory T cells. Cancer Immunol Res 2016;4(3):194–203.
[10] Sobottka, Nowak B, Frei AL M, et al. Establishing standardized immune phenotyping of metastatic melanoma by digital pathology. Lab Invest 2021;101(12):1561–70.
[11] Massi D, Rulli E, Cossa M, et al. The density and spatial tissue distribution of $CD8^+$ and $CD163^+$ immune cells predict response and outcome in melanoma patients receiving MAPK inhibitors. J Immunother Cancer 2019;7(1):308.
[12] De Logu F, Galli F, Nassini R, et al. Digital immunophenotyping predicts disease free and overall survival in early stage melanoma patients. Cells 2021;10(2):422.
[13] de Visser KE, Joyce JA. The evolving tumor microenvironment: from cancer initiation to metastatic outgrowth. Cancer Cell 2023;41(3):374–403.
[14] Reina-Campos M, Moscat J, Diaz-Meco M. Metabolism shapes the tumor microenvironment. Curr Opin Cell Biol 2017;48:47–53.

[15] Chen Z, Han F, Du Y, et al. Hypoxic microenvironment in cancer: molecular mechanisms and therapeutic interventions. Signal Transduct Target Ther 2023;8 (1):70.
[16] Chen G, Wu K, Li H, et al. Role of hypoxia in the tumor microenvironment and targeted therapy. Front Oncol 2022;12:961637.
[17] Baghban, Roshangar R, Jahanban-Esfahlan L, et al. Tumor microenvironment complexity and therapeutic implications at a glance. Cell Commun Signal 2020;18 (1):59.
[18] Conway JW, Rawson RV, Lo S, et al. Unveiling the tumor immune microenvironment of organ-specific melanoma metastatic sites. J Immunother Cancer 2022;10(9):e004884.
[19] Kohtamäki L, Leivonen SK, Mäkelä S, et al. Intra-patient evolution of tumor microenvironment in the pathogenesis of treatment-naïve metastatic melanoma patients. Acta Oncol 2023;62(9):1008–13.
[20] Falcone I., Conciatori F., Bazzichetto C., et al. Tumor microenvironment: implications in melanoma resistance to targeted therapy and immunotherapy. Cancers (Basel). 202; 12(10):2870.
[21] Wilmott JS, Long GV, Howle JR, Haydu LE, Sharma RN, Thompson JF, Kefford RF, Hersey P, Scolyer RA. Selective BRAF inhibitors induce marked T-cell infiltration into human metastatic melanoma. Clin Cancer Res 2012;18(5):1386–94.
[22] Boni A, Cogdill AP, Dang P, et al. Selective BRAFV600E inhibition enhances T-cell recognition of melanoma without affecting lymphocyte function. Cancer Res 2010; 70(13):5213–9.
[23] Sumimoto H, Imabayashi F, Iwata T, et al. The BRAF-MAPK signaling pathway is essential for cancer-immune evasion in human melanoma cells. J Exp Med 2006; 203(7):1651–6.
[24] Mandalà M, De Logu F, Merelli B, et al. Immunomodulating property of MAPK inhibitors: from translational knowledge to clinical implementation. Lab Invest 2017;97(2):166–75.
[25] Shabaneh TB, Molodtsov AK, Steinberg SM, et al. Oncogenic $BRAF^{V600E}$ governs regulatory T-cell recruitment during melanoma tumorigenesis. Cancer Res 2018;78 (17):5038–49.
[26] Miao W., Li L., Liu X., et al. A targeted quantitative proteomic method revealed a substantial reprogramming of kinome during melanoma metastasis. Sci Rep. 202; 10(1):2485.
[27] Xu L, Shen SS, Hoshida Y, Subramanian A, et al. Gene expression changes in an animal melanoma model correlate with aggressiveness of human melanoma metastases. Mol Cancer Res 2008;6(5):760–9.